0026-895X/03/6306-1407–1416$7.00
MOLECULAR PHARMACOLOGY
Copyright © 2003 The American Society for Pharmacology and Experimental Therapeutics
Mol Pharmacol 63:1407–1416, 2003

Vol. 63, No. 6
2105/1067742
Printed in U.S.A.

Pharmacological and Biophysical Properties of the Human $P2X_5$ Receptor

XUENONG BO, LIN-HUA JIANG, HEATHER L. WILSON, MIRAN KIM, GEOFFREY BURNSTOCK, ANNMARIE SURPRENANT, and R. ALAN NORTH

Institute of Molecular Physiology, University of Sheffield, Sheffield, United Kingdom (X.B., L.-H.J., H.L.W., M.K., A.S., R.A.N.); and Autonomic Neuroscience Institute, Royal Free and University College Medical School, London, United Kingdom (G.B.)

Received August 26, 2002; accepted March 6, 2003

This article is available online at http://molpharm.aspetjournals.org

ABSTRACT

We constructed a full-length human $P2X_5$ purinoceptor cDNA by incorporating a sequence corresponding to exon 10, which is missing in cDNAs cloned previously from human tissues. We studied the functional properties by patch-clamp recording and fluorescence imaging after expression in human embryonic kidney 293 cells. ATP (1–100 μM; half-maximal current at 4 μM) elicited inward currents at −60 mV; these persisted during brief (2 s) applications but declined during longer applications. The peak current was dependent on the holding potential and showed little rectification; however, both the desensitization during the application and the decline in the current when ATP was washed out were slower at +30 mV than at −60 mV. 2′,3′-*O*-(4-Benzoyl)-benzoyl-ATP and $\alpha\beta$-methylene-ATP mimicked the action of ATP (half-maximal concentrations 6 and 161 μM, respectively). The currents were inhibited by suramin, pyridoxal-5-phosphate-6-azo-2′,4′-disulfonic acid and Brilliant Blue G, with half-maximal inhibition at 3, 0.2, and 0.5 μM, respectively; 2′,3′-*O*-(2′,4′,6′-trinitrophenol)-ATP (1 μM) was ineffective. Removing divalent cations did not significantly alter ATP concentration-response curves. Reversal potential measurements showed that the human $P2X_5$ receptor was permeable to calcium ($P_{Ca}/P_{Na} = 1.5$) and *N*-methyl-D-glucamine (NMDG) ($P_{NMDG}/P_{Na} = 0.4$); it was also permeable to chloride ($P_{Cl}/P_{Na} = 0.5$) but not gluconate ($P_{gluc}/P_{Na} = 0.01$) ions. The permeability to NMDG developed as quickly as the channel opened, in contrast to the $P2X_7$ receptor where the NMDG permeability develops over several seconds. Cells expressing human $P2X_5$ receptors also rapidly accumulated the propidium dye YO-PRO-1 in response to ATP.

A $P2X_5$ subunit cDNA was first isolated from libraries of rat sympathetic ganglia (Collo et al., 1996) and heart (Garcia-Guzman et al., 1996). The RNA is expressed predominantly in heart (Garcia-Guzman et al., 1996) but there is also expression in brain, spinal cord, and adrenal gland (Garcia-Guzman et al., 1996). Immunoreactivity for $P2X_5$ subunits has also been described in developing skeletal muscle of the rat (Meyer et al., 1999; Ryten et al., 2001); recently, the receptor has been implicated in the differentiation of satellite cells into mature multinucleated muscle fibers (Ryten et al., 2002). Mammalian skin (Groschel-Stewart et al., 1999) and endocrine (Glass and Burnstock, 2001) cells also show $P2X_5$ immunoreactivity.

When expressed in HEK293 cells, the rat $P2X_5$ subunit cDNAs gave rise to currents activated by ATP, but these were very small and their properties not extensively studied. The current was elicited by ATP [half-maximal concentration (EC_{50}) about 10 μM] but not by $\alpha\beta$meATP, and it was readily blocked by suramin and PPADS in the 1 to 10 μM concentration range (Collo et al., 1996; Garcia-Guzman et al., 1996). A mouse cDNA has also been cloned and expressed; again, the currents recorded from HEK293 cells were only a few tens of picoamperes and they were not studied in detail (Cox et al., 2001). On the other hand, although these two mammalian receptors do not express well as homomeric channels, their coexpression with $P2X_1$ subunits leads to the appearance of a large membrane current with several distinct properties indicative of a functional $P2X_1/P2X_5$ heteromer (Torres et al., 1998; Lê et al., 1999; Surprenant et al., 2000).

Three nonmammalian vertebrate $P2X_5$ receptor subunits have recently been cloned. The zebrafish (*Danio rerio*) receptor expressed very poorly in HEK293 cells, even though the zebrafish $P2X_4$ receptor gave good currents in parallel exper-

This work was supported by financial assistance from The Wellcome Trust (to A.S.) and AstraZeneca (to R.A.N.).

X.B. and L.-H.J. contributed equally to this work.

[1] Present address: Section of Functional Genomics, Division of Genomic Medicine, University of Sheffield, Royal Hallamshire Hospital, M-floor, Sheffield S10 2JF, United Kingdom.

ABBREVIATIONS: HEK, human embryonic kidney; $\alpha\beta$meATP, $\alpha\beta$-methylene-ATP; PPADS, pyridoxal-5-phosphate-6-azo 2′,4′-disulfonic acid; NMDG, *N*-methyl-D-glucamine; EST, expressed sequence tag; EE, EYMPME epitope; GFP, green fluorescent protein; EGFP, enhanced green fluorescent protein; YO-PRO-1, quinolinium,4-[(3-methyl-2-(3H)-benzoxazolylidene)methyl]-1-[3-(triethylammonio)propyl]di-iodide; BzATP, 2′,3′-*O*-(4 benzoyl)benzoyl-ATP.

iments (Diaz-Hernandez et al., 2002). The bullfrog (*Rana catesbeiana*) receptor cloned from larval skin and the chicken (*Gallus gallus*) receptor cloned from skeletal muscle provided substantive currents in HEK293 cells (Ruppelt et al., 2001) and *Xenopus laevis* oocytes (Bo et al., 2000; Jensik et al., 2001). These nonmammalian receptors share basic pharmacological properties with their mammalian counterparts (e.g., sensitivity to PPADS and suramin) but also exhibit some interesting features not seen in the limited prior studies of the mammalian receptors. For example, Soto's group (Ruppelt et al., 2001) showed that the homomeric chicken $P2X_5$ receptor was significantly permeable to chloride ions, and Jensik et al. (2001) found that the bullfrog receptor became permeable to NMDG and propidium iodide when divalent cations were removed from the solution.

The human $P2X_5$ receptor cDNA was isolated from brain, and its RNA was particularly enriched in thymus and other immune cells (Lê et al., 1997). However, alignment with other members of the P2X families showed that this cDNA lacked exon 10. This form was originally designated $P2X_{5A}$; $P2X_{5B}$ also misses exon 3 (GenBank accession number Q93086). Exon 10 encodes a 22-amino acid segment of protein including much of the second of the two membrane-spanning domains. This cDNA did not encode functional channels, but a chimeric receptor in which the C-terminal region of the rat receptor (starting at the position equivalent to the beginning of exon 10) was joined to the human receptor provided robust ATP-activated currents when expressed in *X. laevis* oocytes (Lê et al., 1997).

The human $P2X_5$ gene occupies about 21 kilobases near the end of the short arm of chromosome 17 (p13.3). We found a sequence corresponding to exon 10 of the $P2X_5$ receptor at the appropriate place in the gene (NCBI contig NT 010692, bases 3,048,945–3,049,010). However, the sequence at the 3′ splice site (GGTGCT*gg*gagt) contains *gg* on the intronic side rather than the gt, which is the consensus for RNA splicing; gt is found at the corresponding position in the mouse (Cox et al., 2001) and chick (Ruppelt et al., 2001) genomic sequences. Remarkably, a single nucleotide polymorphism at precisely this position has been reported (position 3,049,012; NCBI dbSNP ss1321072). In persons with thymidine, exon 10 will be recognized during processing of the $P2X_5$ receptor mRNA and this will be translated to a 'full-length' receptor; persons with guanine at this position will make a receptor that does not include exon 10. Most expressed sequence tags in the dbEST database that contain appropriate fragments of the $P2X_5$ receptor show that exon 10 is missing, but there are cases in which it is present (GenBank accession numbers BG116171, duodenal adenocarcinoma; AW402829, B cell germinal center). In the current release of dbEST, 12 ESTs are missing exon 10, and two ESTs contain it; this provides a crude estimate of the frequency of the G > T polymorphism of 14%.

We therefore undertook to construct and express a full-length human $P2X_5$ receptor cDNA. This seemed to be a worthwhile goal in view of 1) the widespread tissue distribution of the subunit, 2) the limited expression studies of other mammalian homomeric $P2X_5$ receptors, 3) the interesting properties of the channels formed by the chick and bullfrog subunits, and 4) the indication from genomic sequence and ESTs that the 'exon 10-containing' receptor will in fact be made by a subset of individuals.

Materials and Methods

Construction of Full-Length Human $P2X_5$ cDNA. Several $hP2X_5$ receptor-related cDNA sequences were identified by a BLAST search of human dbEST database with the coding region of $hP2X_5$ cDNA (GenBank accession number AF016709). One of the clones from a human lung small cell carcinoma was purchased (GenBank accession number BE791872; Incyte Genomics Inc., Palo Alto, CA) and sequenced. A TBLASTN search of human genomic DNA with the exon 10 sequence of rat $P2X_5$ cDNA identified a corresponding sequence (AF168787, translation is Ala^{325}-Gly-Lys-Phe-Ser-Ile-Ile-Pro-Thr-Ile-Ile-Asn-Val-Gly-Ser-Gly-Val-Ala-Leu-Met-Gly-Ala, which has three conservative differences from the equivalent rat sequence) (Fig. 1A). To produce the full-length $hP2X_5$ receptor, the cDNA of the EST clone was subcloned from the original pOTB7 vector into pRS7T vector with *Eco*RI and *Xho*I. The 5′ nontranslated region was removed by digesting with *Nco*I and the plasmid was religated. To insert the missing exon 10 into the modified EST clone, the following four primers were used for overlap extension-based mutagenesis: 5′-cccaccatcatcaacgtgggctct-ggggtggcgctcatgggtgctggtgctttcttctgcgacctg, 5′-agagcccacgttgatgatggt-gggaatgatgctgaacttccctgccttgccgttcaccatcacgtc, 5′-tattaccgagacgcagc-cggggt, and 5′-agctcgagtcacgtgctcctgtggggctccag. The fragment obtained with overlap extension, which contained the inserted exon 10, was digested with *Bam*HI and *Xho*I and was used to replace the sequence between *Bam*HI site inside the $P2X_5$ receptor cDNA and the downstream *Xho*I site in the vector. This procedure essentially removed all the 3′ nontranslated region of the EST clone. The full-length coding sequence was subcloned into pcDNA3.1Zeo(+) with *Hin*dIII and *Xho*I.

For comparison of expression levels between human $P2X_5$ and rat $P2X_5$ receptors we used a C-terminal EYMPME (EE) epitope (Kim et al., 2001a). We also truncated the receptors at a position corresponding to the end of exon 11 (Cox et al., 2001); the final amino acid of these constructs was Gly^{378} in both the human and rat receptors; this construct is termed $P2X_5\Delta C$ (Fig. 1A). The full-length and truncated forms of the human receptor were also subcloned into pEGFP-N2 or pEGFP-N3 vectors (BD Biosciences Clontech, Palo Alto, CA) to make $P2X_5$-EGFP and $P2X_5\Delta C$-EGFP. We made point-mutated receptors using QuikChange site-directed mutagenesis kit (Stratagene, La Jolla, CA).

Transient Transfections, GFP Fluorescence, and Immunoblots. The methods were as described in detail previously (Kim et al., 2001a,b). In brief, HEK293 cells were plated in 35-mm Petri dishes, transfected using LipofectAMINE 2000 (Invitrogen) (1 μg of cDNA/2 $\times$ 10^5 cells), and studied 24 to 48 h after transfection. GFP-fused $P2X_5$ receptors were plated on glass coverslips, fixed for 10 min with 4% paraformaldehyde, washed twice with physiological saline, and photographed using a CCD camera and an Olympus BX40 fluorescence microscope. Immunoprecipitation and Western blots were carried out using EE-tagged $P2X_5$ receptors as described previously (Kim et al., 2001a,b). Protein was bound to anti-EE monoclonal antibody (BabCo, Richmond, CA) and precipitated with γ-bind G-Sepharose (Amersham Biosciences, Uppsala, Sweden). Immune complex was then dissociated from γ-bind G-Sepharose, applied to SDS-PAGE, and blotted with anti-EE polyclonal Ab. Molecular weights were calculated using GeneSnap and GeneTools software (Syngene, Cambridge UK).

Electrophysiology and Fluorescent Imaging. Whole-cell patch clamp recordings were obtained using a HEKA EPC9 amplifier and Pulse software (HEKA, Lambrecht Germany) as described previously (Virginio et al., 1998a; Jiang et al., 2001). The internal solution was 172 mM Na^+ 148 mM Cl^-, 10 mM EGTA, and 10 mM HEPES. An agar bridge (3 M KCl) was used for the indifferent electrode. The standard external solution was 151 mM Na^+, 2 mM Ca^{2+}, 1 mM Mg^{2+}, 2 mM K^+, 155 mM Cl^-, 10 mM HEPES, and 13 mM glucose. We used simplified external solutions for measurements of permeability ratios. Solution *147NaCl* contained 151 mM Na^+, 0.3 mM Ca^{2+}, and 148 mM Cl^-; solution *40NaCl* contained 44 mM Na^+, 0.3 mM Ca^{2+}, and 41 mM Cl^-; solution *110CaCl$_2$* con-

tained 112 mM Ca^{2+} and 220 mM Cl^-; solution *154NMDG* contained 154 mM $NMDG^+$ and 146 mM Cl^-; and solution *147gluc* contained 151 mM Na^+ and 147 mM $gluconate^-$. These solutions also contained HEPES and glucose; osmolarity was 295 to 315 mOsm, and the adjustment of the pH to 7.3 with NaOH, $Ca(OH)_2$, or HCl accounts for the difference between the added salt concentrations and the final ion concentrations. Drug applications were made using the RSC 200 system (Biologic Science Instruments, Grenoble, France). In these experiments, solution exchange times were estimated from changes in junction potentials when a solution of 147 mM potassium gluconate was applied; these averaged 80 ms. Antagonists were applied for 1 to 4 min before, and throughout, agonist applications; agonist applications were repeated at 2- to 4-min intervals.

For reversal potential measurements, the whole-cell configuration was established in standard external solution and the external solution was changed to solution *147NaCl*; the reversal potential was obtained by a ramp voltage command (−120 to 40 mV; 1-s duration). The solution was then exchanged with one of solutions described above, and the reversal potential was measured again. The reversal potentials reported have been corrected for liquid junction potentials, which were calculated using Henderson's equation (Ives and Janz, 1961), and in any case did not exceed 4 mV. The permeability ratios (P_X/P_{Na}) were derived from the reversal potentials (E_{rev}) as follows [where $x = E_{rev}\,F/R\,T$ (F is the Faraday constant, R is the gas constant, and T is the absolute temperature)]:

For solution *40NaCl*: $P_{Cl}/P_{Na} = \{(1 - exp(-x))\ ([Na]_o - [Na]_i\ exp(x))\}/\{([Cl]_i exp(-x) - [Cl]_o)\ (1 - exp(x))\}$. The estimate of P_{Cl}/P_{Na} (0.52) was used for further estimates of permeability ratios.

For solution *110CaCl₂*: $P_{Ca}/P_{Na} = (A + B)/4[Ca]_o$ where $A = \{[Na]_i\ exp(x)\ (1 + \exp(x))\}$ and $B = P_{Cl}/P_{Na}\ (1 + exp(x))\ ([Cl]_o\ exp(x) - [Cl]_i)$.

For solution *147NMDG*: $P_{NMDG}/P_{Na} = (C + D)/E$ where $C = ([Na]_i\ exp(x))/(1 - exp(x))$, $D = P_{Cl}/P_{Na}\ ([Cl]_i exp(-x) - [Cl]_o)/(1 - exp(-x))$ and $E = [NMDG]_o/(1 - exp(x))$.

For solution *147gluc*: $P_{gluc}/P_{Na} = (C+D)/F$ where $F = [gluc]_o/(1 - exp(-x))$.

Ion concentrations were converted to activities using the following coefficients: $\gamma_{Na} = 0.75$, $\gamma_{Cl} = 0.75$, $\gamma_{Ca} = 0.28$, $\gamma_{NMDG} = 0.81$, and $\gamma_{gluc} = 0.81$.

YO-PRO-1 fluorescence was measured as described previously (Virginio et al., 1999a); we used a Zeiss Axiovert 100 and Fluar 20× objective with Photonics monochrometer imaging (Photonics, Germany).

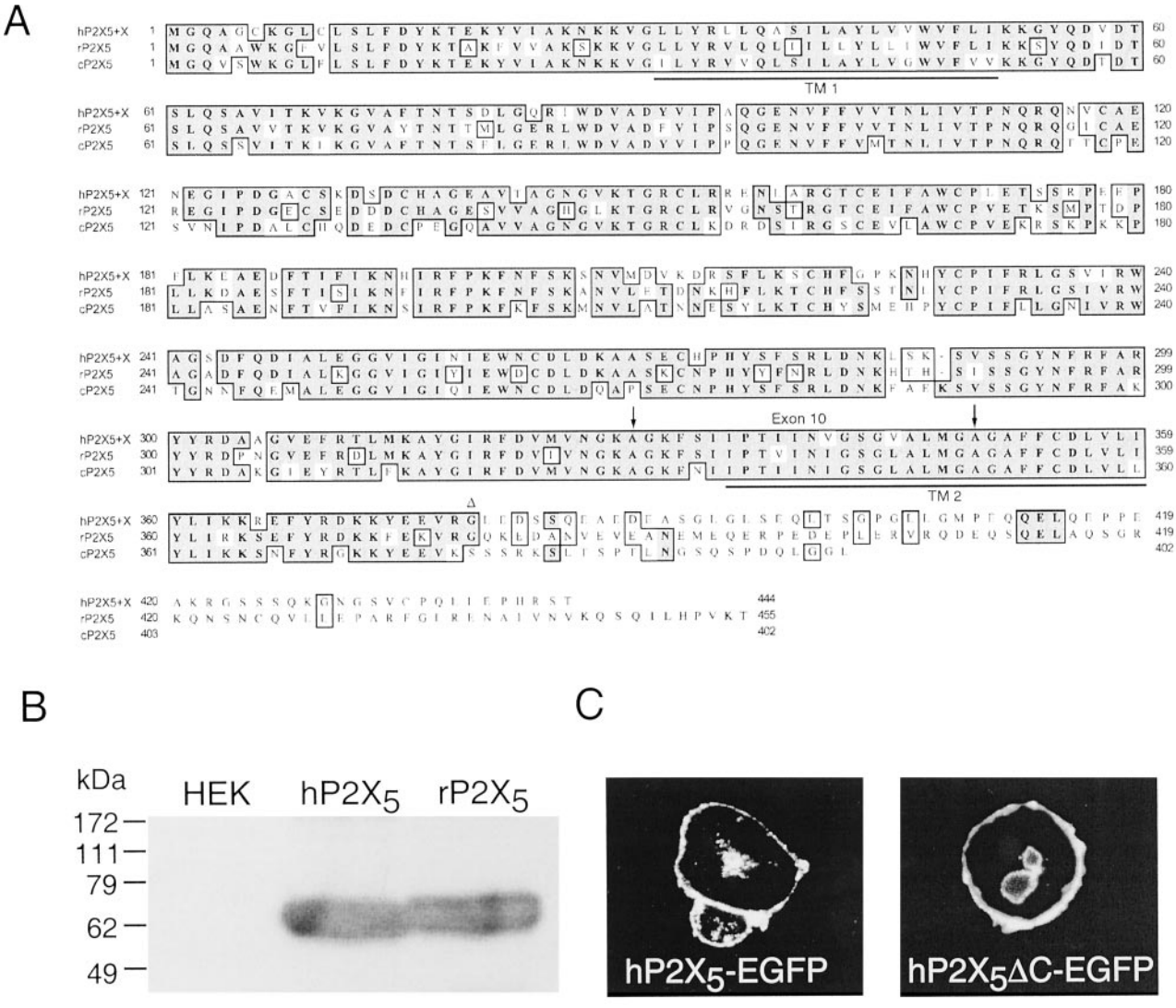

Fig. 1. Construction and expression of full-length $hP2X_5$ receptor. A, amino acid sequence alignment of human, rat, and chick $P2X_5$ receptors. Transmembrane domains (TM1, TM2) are underlined, exon 10 is indicated by two arrows, and the C-terminal truncation site on rat and human $P2X_5$ is indicated by Δ. B, Western blot of epitope-tagged human and rat $P2X_5$ receptors; lane 1 is untransfected HEK cells. C, GFP fluorescence in HEK293 cells transfected with full-length $hP2X_5$-EGFP or C-terminal truncated $hP2X_5$-EGFP. Both proteins localize to the plasma membrane.

Data Analysis. Figures show mean ± S.E.M for number of cells and curves fitted from pooled data using Kaleidagraph (Synergy Software, Reading PA). Onset and offset of ATP action were approximated by single exponentials of time constant τ_{on} and τ_{off}; the corresponding rate constants ($k_1 = \{(1/\tau_{on}) - k_{-1}\}/[ATP]$ and $k_{-1} = 1/\tau_{off}$) were assumed to be related to membrane potential by an expression of the form $k(V) = k(0)\ exp(-z\ \delta\ V\ F/R\ T)$ where V is the membrane potential, δ is the fraction of the membrane electric field acting on a sensor of valence z, and $k(0)$ is the rate constant at 0 mV. Agonist concentration-response curves were fit by $I/I_{max} = 100\ ([A]^{nH}/([A]^{nH} + EC_{50}{}^{nH}))$, where I is the peak current evoked by agonist concentration [A] expressed as percentage of maximal current evoked by ATP, n_H is the Hill coefficient, and EC_{50} is the half-maximal agonist concentration. Antagonist concentration-inhibition curves were fit to $I/I_o = 100\ ([B]^{nH}/([B]^{nH} + EC_{50}{}^{nH}))$, where I is the peak current at a given antagonist concentration [B] as a percentage of current in absence of antagonist (I_o) and IC_{50} is the antagonist concentration that inhibits agonist current by 50%. Numerical estimates of EC_{50} and IC_{50} were obtained by curve-fitting to individual cells.

Results

Expression of Human $P2X_5$ Receptor. Transfection of HEK293 cells with either human $P2X_5$ or rat $P2X_5$ receptor cDNAs resulted, within 1 to 2 days, in strong expression of the protein (Fig. 1, B and C). Immunoblotting of proteins from these cells showed single bands at 61 and 62 kDa, respectively (Fig. 1B), which is appropriate to glycosylated proteins with calculated molecular masses of the two $P2X_5$ proteins (51 and 52 kDa). This was primarily localized to the plasma membrane by immunocytochemistry (Fig. 1C). Although Western blotting showed equivalent protein expression of the rat and human $P2X_5$ receptor, currents evoked by ATP at the rat $P2X_5$ receptor were extremely small (<50 pA in these experiments; see also Collo et al., 1996; Garcia-Guzman et al., 1996), whereas ATP-evoked currents at the human $P2X_5$ receptor were large (1–5 nA at −60 mV) (Fig. 2). We observed no significant differences in the immunohistochemistry or in the ATP-evoked currents between HEK293 cells transfected with an epitope-tagged human $P2X_5$ receptor ($hP2X_5$-EE) or with an EGFP-fused $hP2X_5$ receptor ($hP2X_5$-EGFP) (Fig. 1C); therefore, we have included some experiments with these constructs in the results of the functional experiments.

Agonist and Antagonist Actions at Human $P2X_5$ Receptor. Application of ATP (0.3–3 μM; 1–5 s) evoked inward currents (at −60 mV) that were sustained; the currents elicited by higher concentrations declined during the application (Fig. 2A). Concentration-response curves for ATP, BzATP, and αβmeATP yielded EC_{50} values of 4.1 ± 0.5 (n = 5), 5.7 ± 0.9 (n = 5), and 161 ± 35 μM (n = 4), respectively (Fig. 2B). BzATP, αβmeATP, and 2-methylthio-ATP elicited >85% of the maximal ATP current; adenosine-5′-*O*-(3-thio)triphosphate, ADP, and βγ-methylene-ATP acted as less full agonists (Fig. 2C). Thus, the sensitivity to αβmeATP is much greater than that observed for the rat $P2X_5$ receptor (no effect of 300 μM αβmeATP; Collo et al., 1996), somewhat greater than that found for the rat $P2X_2$ receptor (Spelta et al., 2002) but considerably less than that reported for $P2X_1$, $P2X_3$, $P2X_{2/3}$, and $rP2X_{1/5}$ receptors (see North and Surprenant, 2000).

PPADS, Brilliant Blue G (BBG), and suramin inhibited the ATP-evoked current; this was concentration-dependent with IC_{50} values of 0.2 ± 0.02 (n = 3), 0.53 ± 0.04 (n = 3), and 2.9 ± 0.4 (n = 5) μM, respectively (Fig. 2D). The sensitivity to inhibition by PPADS observed for the human $P2X_5$ receptor is about 10-fold higher than previously reported for other heterologously expressed P2X receptors (North and Surprenant, 2000). The inhibition by BBG is intermediate between the high sensitivity of the rat and human $P2X_7$ receptor (IC_{50}, 10 and 200 nM, respectively) and the very low sensitivity of the other P2X receptors (IC_{50} values >5–10 μM) (Jiang et al., 2000). 2′,3′-*O*-(2′,4′,6′-Trinitrophenol)-ATP, which is a nanomolar affinity antagonist at the $P2X_1$, $P2X_3$, and $P2X_{2/3}$ receptors (Virginio et al., 1998b; North and Surprenant, 2000), only minimally inhibited the ATP-evoked currents at the human $P2X_5$ receptor (11 ± 5% inhibition at 1 μM, n = 3).

Kinetics of Agonist Action. There were some features of the action of ATP that differed from those observed previously at other P2X receptors. First, the onset of the current was slower. We measured τ_{on} at the human $P2X_5$ and rat $P2X_2$ receptors under the similar conditions using near-maximal ATP concentrations (10 and 30 μM, respectively; holding potential, −60 mV); the values were 410 ± 50 ms (n = 8) and 161 ± 10 ms (n = 4). The rate of onset of the current showed little if any dependence on membrane potential (Fig. 3A), but the rate of the offset of the response upon removal of agonist was almost 10-fold slower at +30 mV than at −60 mV (Fig. 3, B and C). The offset rate constant was 0.2/s at 0 mV, and the fraction of the membrane field sensed by the channel closing (assuming a monovalent sensor) was 0.6. The offset of the current at the rat $P2X_2$ receptor was some 10 times faster and was not voltage-dependent (τ_{off} was about 300 ms at all potentials; Fig. 3C).

The desensitization of the current that occurred with longer agonist applications was also voltage-dependent (Fig. 3A). At a holding potential of −30 mV, the current at the end

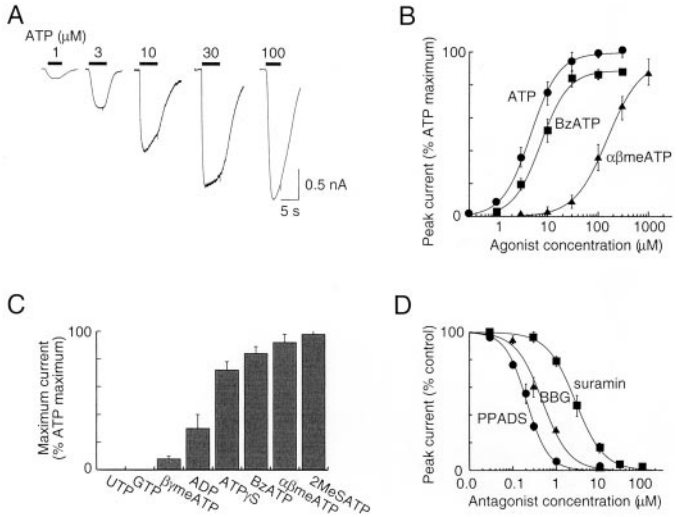

Fig. 2. Pharmacological properties of full-length human $P2X_5$ receptor. A, inward currents recorded at −60 mV in response to 5-s applications of ATP. B, agonist concentration-response curves for ATP, BzATP, and αβmeATP. Results are plotted as percentage of maximum ATP current recorded in each cell; each point is mean ± S.E.M. (n = 4–12 points). C, maximum currents caused by various agonists (100 μM) relative to that evoked by ATP; each bar is mean ± S.E.M. (n = 3–12). D, antagonist inhibition curves for PPADS, Brilliant Blue G, and suramin at human $P2X_5$ receptor; ATP (10 μM) was the agonist. Each point is mean ± S.E.M. (n = 3–8).

of a 10-s application of ATP (3 μM) had declined to 48 ± 11% (n = 6) of its peak value; the corresponding value at +30 mV was 86 ± 3% (n = 8). The ATP-evoked current at the chick and bullfrog $P2X_5$ receptor shows rapid desensitization (at −60 mV) that is prevented by removal of external calcium (Bo et al., 2000; Ruppelt et al., 2001). However, in the present study on the human $P2X_5$ receptor, removal of calcium from the superfusion solution did not alter the ATP concentration-response curve (n = 3), the onset or offset kinetics of the ATP current at any membrane potential (n = 6), or the desensitization during the continued presence of agonist (n = 3).

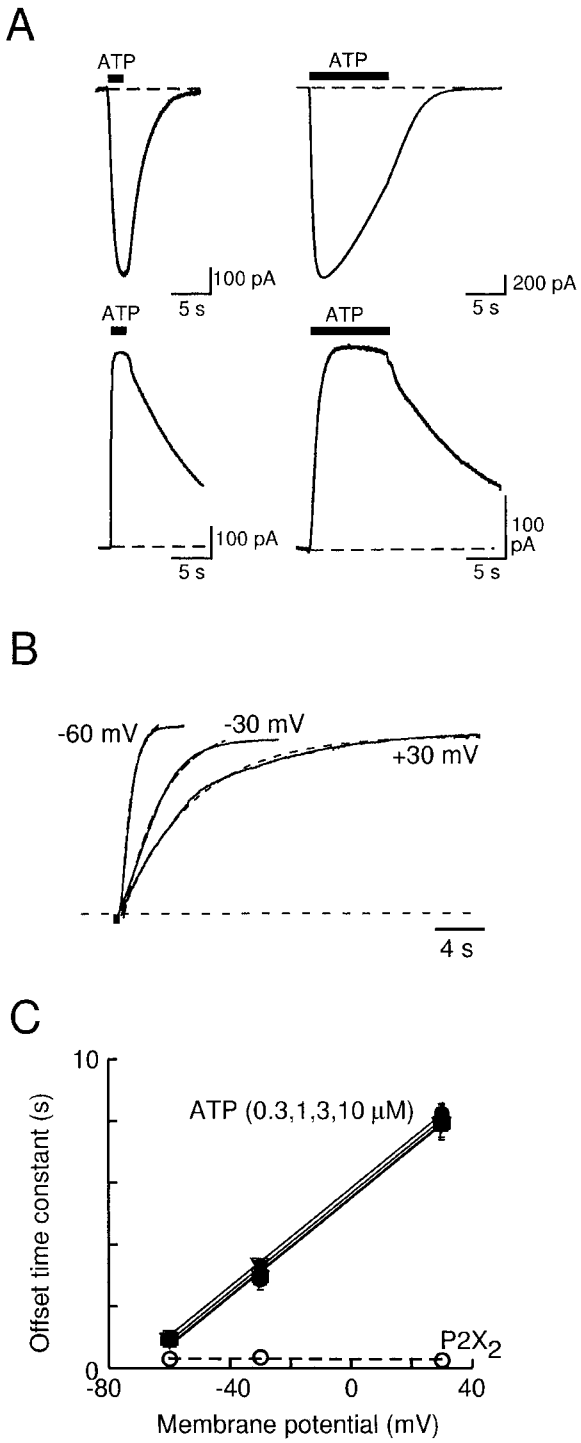

Fig. 3. Kinetics of human $P2X_5$-mediated currents. A, upper traces show inward currents (holding potential −30 mV) in response to 2- and 10-s applications of ATP (3 μM, approximately EC_{50}). Lower traces show typical outward currents at +30 mV. B, offset of response to ATP (3 μM) at −60, −30, and 30 mV (current at +30 mV inverted; currents scaled for comparison); broken lines are exponential fits (time constants 1, 3.3, and 6.3 s). C, summary data from experiments such as those shown in B. ○, results from parallel experiments on rat $P2X_2$ receptor; ATP was applied at 30 μM, which is close to the EC_{90} (n = 5 for all points).

Ion Permeability. We investigated the ion permeability at the human $P2X_5$ receptor by measuring reversal potentials with patch pipettes containing 147 mM NaCl, and changing the composition of the external solutions. The reversal potential in solution *147NaCl* was −0.4 ± 1.1 mV (n = 6). We first estimated P_{Cl}/P_{Na} with solution *40NaCl* (Fig. 4). Table 1 shows that the shift in reversal potential (−12 mV) was much less than expected for a chloride-impermeable channel (the theoretical value would be −33 mV). Thus, the human $P2X_5$ receptor has a very significant permeability to chloride ions (P_{Cl}/P_{Na}, 0.5; Table 1), and this was taken into account in estimates of other permeability ratios when chloride ions were present (see *Materials and Methods*). We substituted extracellular chloride with gluconate (solution *147gluc*) and found that gluconate permeability was insignificant (Table 1). By using extracellular NMDG (solution *154NMDG*) and calcium chloride (solution *110CaCl$_2$*), we found that that the human $P2X_5$ receptor was quite permeable to NMDG (P_{NMDG}/P_{Na}, 0.37) and calcium (P_{Ca}/P_{Na}, 1.5) (Fig. 4; Table 1). Parallel experiments were carried out for direct comparison on cells expressing the rat $P2X_2$ and $P2X_{2/3}$ receptors; we found that these receptors have very low permeability to NMDG ($P_{NMDG}/P_{Na} < 0.05$) (see also Virginio et al., 1999b) and chloride ($P_{Cl}/P_{Na} < 0.02$) ions (Table 1).

The significant difference in chloride permeability between the human $P2X_5$ receptor and the $P2X_2$ receptor led us to search for amino acid residues in or around the transmembrane domains that might differ between the two channels. A possible candidate is Lys^{52} of the $hP2X_5$ receptor, which corresponds in position to Gln^{52} of the rat $P2X_2$ receptor; $P2X_5$ receptors are unusual in having lysine in this position, where $P2X_1$, $P2X_2$, $P2X_3$, $P2X_4$, and $P2X_7$ subunits have a negatively charged side chain (Gln, Asp, Asn, or Glu). This

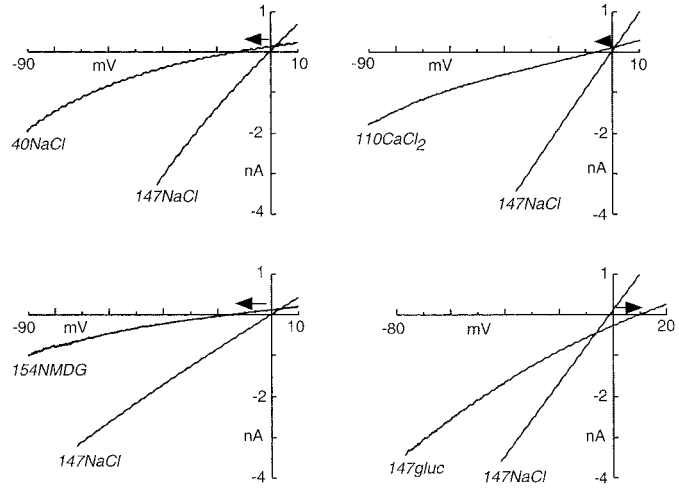

Fig. 4. Human $P2X_5$ receptor ion channel is permeable to large cations and chloride. Currents in response to ramp voltage commands in external solutions containing (each control) *147NaCl*, and solution *40NaCl*, solution *110CaCl$_2$*, solution *147NMDG*, and solution *147gluc*. In each case, arrows indicate change in reversal potential on changing from *147NaCl*.

position is at the outer end of the first transmembrane domain, and we speculated that the difference in charge might contribute to the difference in anion permeability. We reversed the charge by mutagenesis and measured the P_{Cl}/P_{Na} ratios. The value for the human $P2X_5$ receptor was not different from wild type, and the rat $P2X_2$ receptor with the complementary mutation [Q52K] remained impermeable to chloride (Table 1).

In the case of the $P2X_7$ receptor (Surprenant et al., 1996; Virginio et al., 1999b), the permeability to NMDG is very low at the beginning of the ATP application and progressively increases over several seconds. Indeed, when the application of agonist is kept brief (≈2 s), there is no significant permeability to NMDG (Surprenant et al., 1996). NMDG permeability has also been found for the $P2X_2$ and $P2X_4$ receptor, but in these cases, it also develops during several seconds of agonist application (Khakh et al., 1999; Virginio et al., 1999b). This progressive increase in permeability is detected as a time-dependent change in reversal potential during a sustained application of agonist. We therefore directly compared the kinetics of NMDG permeability at the rat $P2X_7$ and the human $P2X_5$ receptors under the same conditions (Fig. 5). As reported previously (Virginio et al., 1999a,b), the reversal potential in NMDG chloride shifted over an exponential time course from about −90 mV ($P_{NMDG}/P_{Na} < 0.02$) in the first several seconds of agonist application to a steady-state value of approximately −21 mV (P_{NMDG}/P_{Na} 0.25) after 30 s (Fig. 5, B and C). However, for the human $P2X_5$ receptor, the reversal potential in NMDG chloride was −15 ± 2 mV ($n = 7$) as soon as it was feasible to measure it (1–4 s after ATP application) and did not change during the subsequent 30 s of receptor stimulation (Fig. 5, A and C). Indeed, the onset kinetics of the inward current were no different in solutions containing sodium or NMDG as the only extracellular cation (Figs. 3 and 5), indicating that, within our resolution, the channel is NMDG-permeable from the time at which it opens. The permeability to NMDG was observed in external solutions containing no divalent cations (used for more accurate measurement of reversal potentials), but it was also observed in solutions containing NMDG, calcium (2 mM), and magnesium (1 mM) ($n = 4$).

YO-PRO-1 Permeability of Human $P2X_5$ Receptor. YO-PRO-1 is a propidium dye that becomes fluorescent when it intercalates nucleic acid. We followed its entry into cells by fluorescence imaging. We compared the rate of YO-PRO-1 uptake induced by ATP and BzATP at the human $P2X_5$ and rat $P2X_7$ receptors (Fig. 6). Neither BzATP (100 μM) nor ATP (1 mM) evoked any YO-PRO-1 fluorescence in mock-transfected HEK293 cells ($n > 40$ cells from three separate experiments; Fig. 6A). The absolute fluorescence measured 60 s after the addition of a maximal concentration of either ATP or BzATP was ~2-fold greater at the human $P2X_5$ receptor (Fig. 6A), whereas the rate of YO-PRO-1 uptake was almost 4-fold greater at the human $P2X_5$ receptor (Fig. 6B). For the rat $P2X_7$ receptor, the rate of YO-PRO-1 uptake was greater when the external solutions contained no divalent cations (see Surprenant et al., 1996), but this difference was not present for the $P2X_5$ receptor (Fig. 6B).

Comparison of Human and Rat $P2X_5$ Receptors. We were struck by the robust expression of ionic currents by HEK cells transfected with the human $P2X_5$ receptor, compared with the rat $P2X_5$ receptor (Collo et al., 1996; Garcia-Guzman et al., 1996). Moreover, there were clear functional

TABLE 1

Reversal potential (E_{rev}) and calculated permeability ratios (P_X/P_{Na}) for ATP-evoked currents. Values are the means ± S.E.M. for the number of cells indicated in parentheses

Solution	X	E_{rev}	P_X/P_{Na}
		mV	
Wild-type human $P2X_5$			
147NaCl	Na^+	−0.4 ± 1.1 (6)	1
40NaCl	Cl^-	−11.9 ± 1.0 (5)	0.52
154NMDG	NMDG	−15.4 ± 1.7 (7)	0.37
110CaCl$_2$	Ca^{2+}	−6.9 ± 1.1 (3)	1.49
147gluc	Gluconate	6.7 ± 1.2 (4)	0.01
Human $P2X_5$[K52Q]			
40NaCl	Cl^-	−11.7 ± 1.0 (3)	0.53
Wild-type rat $P2X_2$			
40NaCl	Cl^-	−35.6 ± 0.5 (3)	0
Rat $P2X_2$[Q52K]			
40NaCl	Cl^-	−35.1 ± 2.1 (3)	0

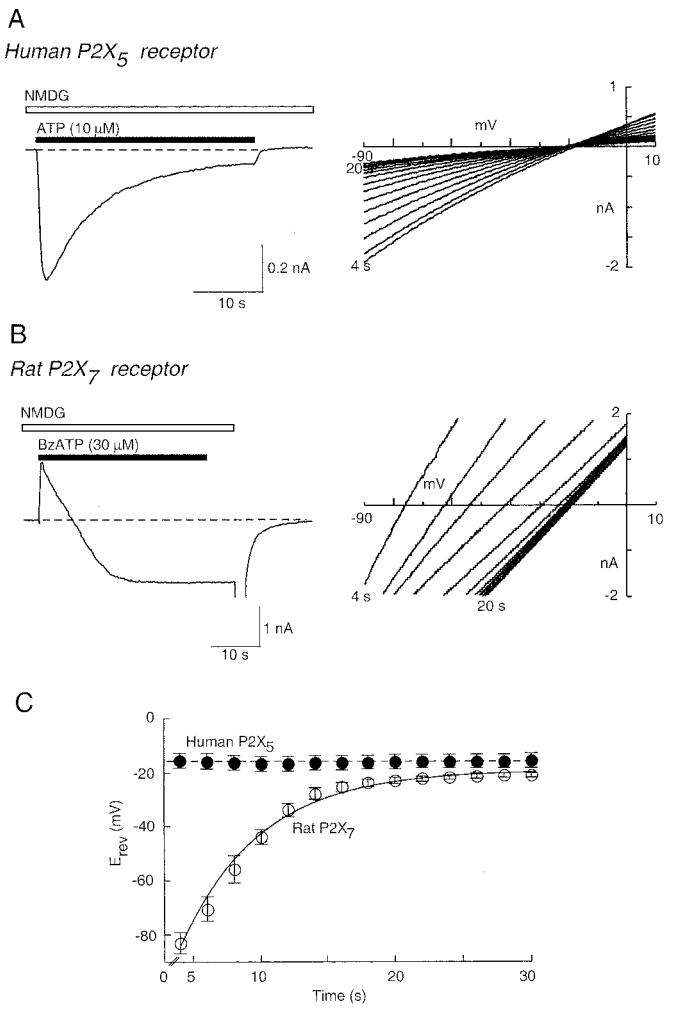

Fig. 5. NMDG permeability is not time-dependent at the human $P2X_5$ receptor. A, left, with NMDG as the extracellular cation, application of ATP evokes an inward current that declines during 30 s. Holding potential, −60 mV. Right, the reversal potential of the current remains at about −15 mV throughout. B, left, a similar experiment on a cell expressing rat $P2X_7$ receptor. The current is initially outward, because the reversal potential is negative to the holding potential (−60 mV). Right, the reversal potential shifts in a positive direction during 20 s of BzATP application. C, summary of results from experiments shown in A and B [$n = 4$ (human $P2X_5$), $n = 3$ (rat $P2X_7$)].

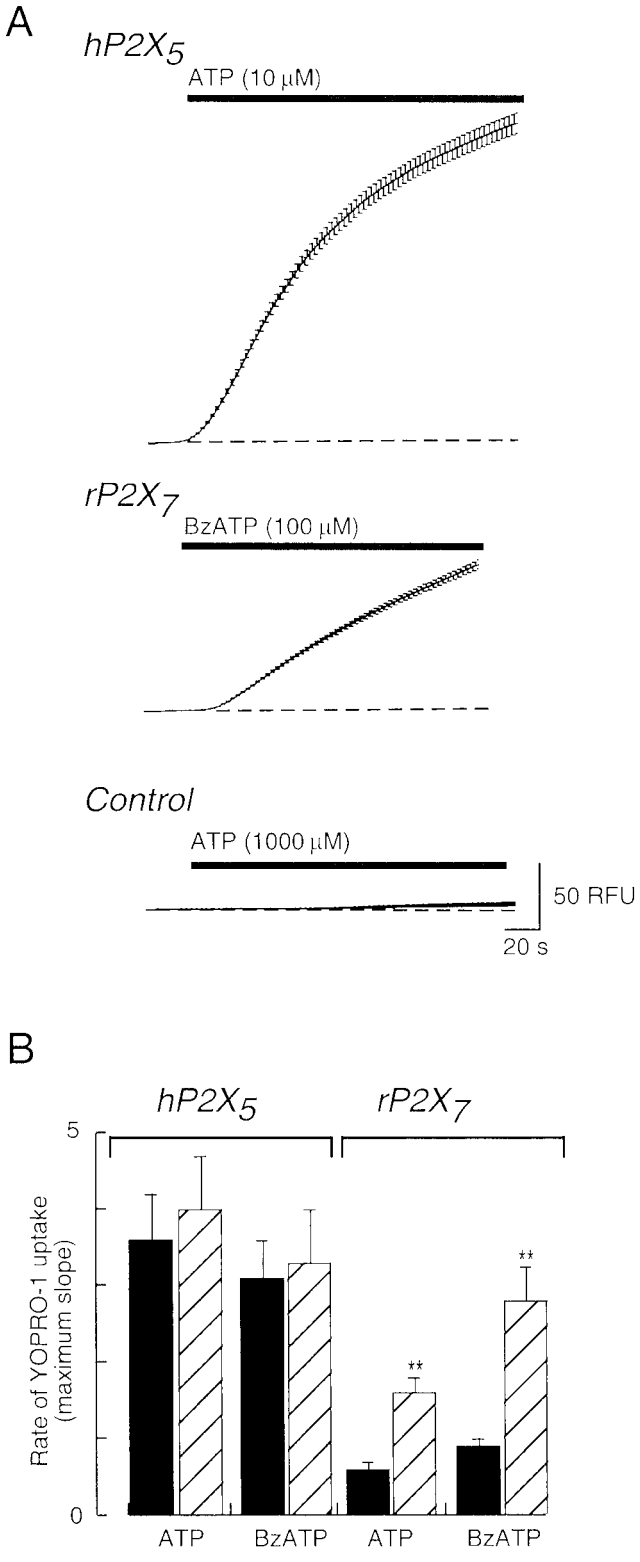

Fig. 6. Uptake of YO-PRO-1 by cells expressing human P2X$_5$ receptors. A, fluorescence of individual HEK cells was measured, and average values are plotted with S.E.M. Top, increase in fluorescence occurring during application of ATP as shown. Middle, a similar experiment on HEK cells expressing rat P2X$_7$ receptors. Bottom, a similar experiment on mock-transfected HEK cells. B, summary of results from experiments such as those shown in A. ■, experiments in standard extracellular solution; ▨, experiments in solution containing 0.3 mM calcium and 0 mM magnesium. Agonist concentrations used were hP2X$_5$, 10 μM ATP, 100 μM BzATP; rP2X$_7$, 1 mM ATP, 100 μM BzATP (n = 3–5). **, $p < 0.05$.

differences between the properties of the two homomers (e.g., increased sensitivity to ATP and $\alpha\beta$meATP, voltage-dependent kinetics). We sought to determine whether these differences might be related to the different C-terminal regions between the two receptors (Fig. 1A).

In general, the C-terminal regions of the P2X receptors show little conservation of sequence among the seven subtypes, but within each subtype, there is significant homology among species orthologs. However, for the P2X$_5$ receptor, the C-terminal regions are related in sequence only between rat and mouse but not in the case of bullfrog, zebrafish, chicken, and human; in these species, all relatedness ends at the splice site between exons 11 and 12 (Cox et al., 2001). We therefore compared the properties of the human and rat receptors truncated at this point (Fig. 1A). Both truncated receptors (with C-terminal EGFP fusions) localized to the plasma membrane in a manner similar to that of the wild-type receptors, although they both showed a lower level of immunofluorescence than did the wild type. The maximum current amplitudes were slightly lower in each of the truncated receptors compared with their respective wild-type receptors. The maximum ATP-evoked currents at wild-type and truncated rat P2X$_5$ receptors were 49 ± 14 pA and 28 ± 9 pA (n = 10 each); at wild-type and truncated human P2X$_5$ receptor, maximum currents were 2.9 ± 0.5 and 0.95 ± 0.1 nA (n = 9 each). However, no other significant differences in the functional properties were observed. The EC$_{50}$ for ATP was 3.3 ± 0.2 μM (n = 3) at the truncated human P2X$_5$ receptor; $\alpha\beta$meATP (100 μM) did not evoke any current at the truncated rat P2X$_5$ receptor but was almost a full agonist at the truncated human P2X$_5$ receptor (n = 4), and the truncated human P2X$_5$ receptor also showed a voltage-dependence time course of current offset (n = 5).

There are three amino acid differences between human and rat receptors in the part of the protein encoded by exon 10. We made a chimeric receptor in which the sequence coded by exon 10 from the rat receptor was used to replace the equivalent sequence of the human receptor. The resulting human receptor [P2X$_5$, V337I/V340I/V344L] had properties indistinguishable from those of the human P2X$_5$ receptor. There are only minor differences between the human and rat P2X$_5$ receptors in the regions before and including the first transmembrane domain (1–50) and between the end of the second transmembrane domain and the truncation point (334–379); it is likely that different residues in the ectodomains may account for the different properties.

Discussion

Our work shows that a P2X$_5$ receptor containing all 13 exons encoded by the human gene expresses well in HEK293 cells and produces robust currents in response to ATP. It has previously been well documented that the form of the receptor that does not contain exon 10 can not form homomeric channels despite apparently good membrane expression (Lê et al., 1997). Human tissues seem to contain more P2X receptor forms that are spliced so as to produce nonfunctional proteins than are found in rodent orthologs (e.g., P2X$_2$, Lynch et al., 1999; P2X$_6$, Urano et al., 1997; see North, 2002); this might reflect a loss of function during evolution. The presence of a polymorphism at a critical position in the human P2X$_5$ gene strongly indicates that a subset of humans will

process and translate their RNA to make the protein that we have expressed. Presumably, mice and chickens also make a protein corresponding to the 'full-length' 13-exon form (see Introduction).

When expressed in mammalian cells or oocytes from cDNAs, the human (this study), chick (Bo et al., 2000; Ruppelt et al., 2001), and bullfrog (Jensik et al., 2001) $P2X_5$ receptors express well; it is less clear why currents at the rat (this study; Collo et al., 1996; Garcia-Guzman et al., 1996), mouse (Cox et al., 2001), and zebrafish receptors (Diaz-Hernandez et al., 2002) do not. The rat sequence contains in its C terminus a sequence Arg^{404}-Val-Arg; this is similar in the mouse (Arg^{404}-Val-His). The RXR motif is a well known endoplasmic reticulum retention motif and has been implicated in the trafficking of several ion channels to the plasma membrane (Ma and Jan, 2002). We mutated this sequence to Ala-Ala-Ala in the rat $P2X_5$ receptor but found that the currents recorded from transfected HEK293 cells were still very small (L.-H. Jiang, unpublished observations). In any event, using Western blotting and immunohistochemistry, we detected no obvious difference between the expression of rat and human $P2X_5$ receptors.

Compared with other homomeric P2X receptors, the pharmacological profile of the human $P2X_5$ receptor is most similar to the $P2X_2$ receptor (North and Surprenant, 2000). It is rather more sensitive to the agonists ATP ($EC_{50} \approx 5\ \mu M$) and $\alpha\beta$meATP ($EC_{50} \approx 150\ \mu M$) and the antagonist PPADS ($IC_{50} < 1\ \mu M$). The current shows much less rectification than is observed for the $P2X_2$ receptor; in this respect, it is more similar to homomeric $P2X_4$ and $P2X_7$ receptors (see North, 2002). Compared with $P2X_5$ receptors from other species [chick (Bo et al., 2000; Ruppelt et al., 2001) and bullfrog (Jensik et al., 2001)], the most noticeable difference is the relatively slower desensitization of the current at the human receptor. As seen for the chick receptor (Ruppelt et al., 2001), we observed that holding the membrane potential at positive could largely prevent desensitization. In the chick, calcium entry might contribute to the desensitization because removing the extracellular calcium ions also prevented it; we did not find this to be the case for the human $P2X_5$ receptor.

The kinetics of channel opening, as best we could estimate with the present approach, corresponded to a macroscopic k_{+1} of 1 μM/s, which is approximately similar to that observed for $P2X_2$ receptors (Ding and Sachs, 1999); this rate showed only little voltage dependence. On the other hand, the rate of decline of the current ranged from 1/s at −60 mV to 0.15/s at +30 mV (Fig. 2). This is in contrast to the rat $P2X_2$ receptor, where the offset of current shows little or no voltage-dependence (Fig. 2). Taken together, the results indicate that depolarized membrane potentials tend to stabilize the human $P2X_5$ receptor in an open state, from which it less easily enters either a desensitized or a closed state.

The permeability of the human $P2X_5$ receptors also shows several unique features. Our measurements of reversal potential when the concentration of extracellular sodium chloride ions was reduced to 40 mM indicate clearly that the channel has substantial chloride permeability ($P_{Cl}/P_{Na} \approx 0.5$). Although it has been widely assumed that P2X receptors are cation-selective, this has often not been tested directly in heterologous expression systems. In the present study, we measured the reversal potential for currents at the homomeric $P2X_2$ and heteromeric $P2X_{2/3}$ receptors; these corresponded to the theoretical value for a channel that was impermeable to chloride (Table 1). However, the chick $P2X_5$ receptor has substantial chloride permeability (Ruppelt et al., 2001); their value for P_{Cs}/P_{Cl} of about 2 corresponds well with our present measurement for the human $P2X_5$ receptor (if we assume that $P_{Na} \approx P_{Cs}$). The molecular basis for the relative high permeability to chloride ions is not understood. We noticed a lysine residue near the outer end of the first transmembrane domain of the $P2X_5$ receptor sequences. Of the other P2X receptor subunits, lysine is found only in $P2X_6$ and no permeability information is available; the residue at this position is negatively charged in all the other subunits. However, we were unable to change the chloride permeability by making the appropriate amino acid exchanges at this position. Further knowledge of the anion permeabilities of other (homomeric) P2X receptors would be very helpful to inform the continuation of such a mutagenesis approach to the structural basis of chloride permeability in the human $P2X_5$ channel.

The chloride permeability of the receptor is of particular interest because ATP-activated currents in skeletal muscle have been repeatedly shown to involve a chloride permeability. The original evidence that ATP directly gates the opening of ion channels was based on whole-cell and single-channel recordings from embryonic chick skeletal muscle myotubes (Kolb and Wakelam, 1983). Subsequent studies in chick and frog showed striking developmental regulation of these channels; they disappear during late embryogenesis but reappear in the adult after denervation (Hume and Honig, 1986; Igusa, 1988; Thomas and Hume, 1990a; Thomas et al., 1991; Wells et al., 1995). They are also characterized by both cation permeability and a "substantial increase in chloride permeability" (Hume and Thomas, 1988; Thomas and Hume, 1990b). More recently, chick embryonic skeletal muscle has been shown to express high levels of both $P2X_5$ and $P2X_6$ receptor immunoreactivity, which disappears with development (Meyer et al., 1999).

All these observations might be consistent with the notion that ATP-gated channels in embryonic chick skeletal muscle are composed of $P2X_5$ receptors. There is, however, evidence against the view that the chick receptor is homomeric $P2X_5$. For example, $\alpha\beta$meATP was ineffective at the receptor on muscle cells cultured from 10- or 11-day-old chick embryos (Hume and Honig, 1986; Thomas et al., 1991), whereas it does activate currents in oocytes expressing chick $P2X_5$ receptors ($EC_{50} \approx 30\ \mu M$; Ruppelt et al., 2001). A recent study of ATP-gated currents and intracellular calcium responses in mouse and human skeletal muscle has shown a similar developmental pattern of expression of ATP-activated responses as that observed in chick. The ATP responses activated by ATP and BzATP, but they were activated only very weakly by $\alpha\beta$meATP, and they showed no desensitization (Cseri et al., 2002). As for the chick, these observations suggest that the native mammalian receptor is not likely to be homomeric $P2X_5$. The predominant expression of $P2X_6$ subunits in skeletal muscle (Urano et al., 1997) suggests that possibility that the native receptor might include both $P2X_5$ and $P2X_6$ subunits. A functional role for ATP in the differentiation of rat skeletal muscle has recently been suggested (Ryten et al., 2002). The regeneration of skeletal muscle cells after damage involves resident satellite cells being stimulated to differentiate into myotubes. ATP stimulated this

differentiation, and evidence from immunohistochemistry, reverse transcription-polymerase chain reaction, and electrophysiology strongly implicated involvement of the $P2X_5$ subunit.

The cation permeation properties of the human $P2X_5$ receptor also exhibit some novel features. Permeability to the large cation NMDG has been demonstrated in the case of homomeric $P2X_2$, $P2X_4$, and $P2X_7$ receptors and heteromeric $P2X_{2/3}$ receptors (Virginio et al., 1999a,b; Khakh et al., 1999). The human $P2X_5$ receptor is also permeable to NMDG and the relative permeability (Table 1; $P_{NMDG}/P_{Na} = 0.37$) is similar that described previously for the other receptors. The striking difference for the human $P2X_5$ receptor is that there is no detectable time delay in the development of the NMDG-permeable state. NMDG permeability was also reported for oocytes expressing the bullfrog $P2X_5$ receptor, but this was only observed when the extracellular solution contained no divalent cations (Jensik et al., 2001); it seemed to develop over several seconds, but it is difficult to make direct kinetic comparisons when whole oocytes and small mammalian cells are used as expression systems. YO-PRO-1 is a larger cation than NMDG ($19 \times 10 \times 5.5$ Å compared with $10 \times 7.6 \times 5.5$ Å) and divalent rather than monovalent. It has the advantage that its permeation can be followed in physiological solutions, which is of course not possible when reversal potentials are measured. Human $P2X_5$ receptors exhibit uptake of YO-PRO-1, which is at least as robust as that observed for $P2X_7$ receptors (Fig. 5; also Surprenant et al., 1996; Rassendren et al., 1997). It is not possible to say from these experiments how rapidly the permeability to YO-PRO-1 develops in human $P2X_5$ receptors, but it would seem to be considerably slower than that observed for NMDG.

In summary, we have constructed and expressed a human $P2X_5$ receptor cDNA and characterized some of its pharmacological and biophysical properties. Several of these properties are quite distinct from those of other mammalian P2X receptors. These include a significant permeability to chloride ions, which is of interest because skeletal muscle expresses abundant $P2X_5$ receptor subunits and because ATP-activated currents in skeletal muscle are also chloride-permeable. There is permeability to the large cation NMDG that seems to develop as quickly as that to sodium ions; in other P2X receptors, the increase in NMDG permeability occurs only several seconds after the initial increase in sodium permeability. Finally, we have drawn attention to a single-nucleotide polymorphism that will effectively determine whether an individual organism makes a functioning $P2X_5$ receptor or a nonfunctional form that lacks exon 10.

References

Bo X, Schoepfer R, and Burnstock G (2000) Molecular cloning and characterization of a novel ATP P2X receptor subtype from embryonic chick skeletal muscle. *J Biol Chem* **275:**14401–14407.

Collo G, North RA, Kawashima E, Merlo-Pich E, Neidhart S, Surprenant A, and Buell G (1996) Cloning of $P2X_5$ and $P2X_6$ receptors and the distribution and properties of an extended family of ATP-gated ion channels. *J Neurosci* **16:**2495–2507.

Cox JA, Barmina O, and Voigt MM (2001) Gene structure, chromosomal localization and expression of the mouse ATP-gated ionotropic receptor $P2X_5$ subunit. *Gene* **270:**145–152.

Cseri J, Szappanos H, Szigeti GP, Csernátony Z, Kovács L, and Csernoch L (2002) A purinergic signal tranduction pathway in mammalian skeletal muscle cells in culture. *Pfleug Arch Eur J Physiol* **443:**731–738.

Diaz-Hernandez M, Cox JA, Migita K, Haines W, Egan TM, and Voigt MM (2002) Cloning and characterization of two novel zebrafish P2X receptor subunits. *Biochem Biophys Res Commun* **295:**849–853.

Ding S and Sachs F (1999) Single channel properties of $P2X_2$ purinoceptors. *J Gen Physiol* **113:**695–720.

Garcia-Guzman M, Soto F, Laube B, and Stühmer M (1996) Molecular cloning and functional expression of a novel rat heart P2X purinoceptor. *FEBS Lett* **388:**123–127.

Glass R and Burnstock G (2001) Immunohistochemical identification of cells expressing ATP-gated cation channels (P2X receptors) in the adult rat thyroid. *J Anat* **198:**569–579.

Groschel-Stewart U, Bardini M, Robson T, and Burnstock G (1999) Localisation of $P2X_5$ and $P2X_7$ receptors by immunohistochemistry in rat stratified squamous epithelia. *Cell Tissue Res* **296:**599–605.

Hume RI and Honig MG (1986) Excitatory action of ATP on embryonic chick muscle. *J Neurosci* **6:**681–690.

Hume RI and Thomas SA (1988) Multiple actions of adenosine 5′triphosphate on chick skeletal muscle. *J Physiol* **406:**503–524.

Igusa Y (1988) Adenosine 5′-triphosphate activates acetylcholine receptor channels in cultured Xenopus myotomal muscle cells. *J Physiol* **405:**169–185.

Ives DJG and Janz GJ (1961) Cells with liquid junctions, in *Reference Electrodes: Theory and Practice* (Ives DJG and Janz GJ eds), pp 48–56, Academic Press, New York.

Jiang L-H, Mackenzie AB, North RA, and Surprenant A (2000) Brilliant blue G selectively blocks ATP-gated rat $P2X_7$ receptors. *Mol Pharmacol* **58:**82–88.

Jiang L-H, Rassendren F, Spelta V, Surprenant A, and North RA (2001) Amino acid residues involved in gating identified in the first membrane-spanning domain of the rat $P2X_2$ receptor. *J Biol Chem* **276:**14902–14908.

Jensik PJ, Holbird D, Collard MW, and Cox TC (2001) Cloning and characterization of a functional P2X receptor from larval bullfrog skin. *Am J Physiol* **281:**C954–C962.

Khakh BS, Bao XR, Labarca C, and Lester HA (1999) Neuronal P2X transmitter-gated cation channels change their ion selectivity in seconds. *Nat Neurosci* **2:**322–330.

Kim M, Jiang L-H, Wilson HL, North RA, and Surprenant A (2001a) Proteomic and functional evidence for a $P2X_7$ receptor signalling complex. *EMBO (Eur Mol Biol Organ) J* **20:**6347–6358.

Kim M, Spelta V, Sim JA, North RA, and Surprenant A (2001b) Differential assembly of rat purinergic $P2X_7$ receptor in immune cells of the brain and periphery. *J Biol Chem* **276:**23262–23267.

Kolb HA and Wakelam MJ (1983) Transmitter-like action of ATP on patched membranes of cultured myoblasts and myotubes. *Nature (Lond)* **303:**621–623.

Lê K-T, Boue-Grabot E, Archambault V, and Séguéla P (1999) Functional and biochemical evidence for heteromeric ATP-gated channels composed of $P2X_1$ and $P2X_5$ subunits. *J Biol Chem* **274:**15415–15419.

Lê K-T, Paquet M, Nouel D, Babinski K, and Séguéla P (1997) Primary structure and expression of a naturally truncated human P2X ATP receptor subunit from brain and immune system. *FEBS Lett* **418:**195–199.

Lynch KJ, Touma E, Niforatos W, Kage KL, Burgard EC, Van Bisen T, Kowaluk EA, and Jarvis MF (1999) Molecular and functional characterization of human $P2X_2$ receptors. *Mol Pharmacol* **56:**1171–1181.

Ma D and Jan LY (2002) ER transport signals and trafficking of potassium channels and receptors. *Curr Opin Neurobiol* **12:**287–292.

Meyer MP, Groschel-Stewart U, Robson T, and Burnstock G (1999) Expression of two ATP-gated ion channels, $P2X_5$ and $P2X_6$, in developing chick skeletal muscle. *Dev Dyn* **216:**442–449.

North RA (2002) The molecular physiology of P2X receptors. *Physiol Rev* **82:**1013–1067.

North RA and Surprenant A (2000) Pharmacology of P2X receptors. *Annu Rev Pharmacol Toxicol* **40:**563–580.

Rassendren F, Buell GN, Virginio C, Collo G, North RA, and Surprenant A (1997) The permeabilizing ATP receptor, $P2X_7$. Cloning and expression of a human cDNA. *J Biol Chem* **272:**5482–5486.

Ruppelt A, Ma W, Borchardt K, Silberberg SD, and Soto F (2001) Genomic structure, developmental distribution and functional properties of the chicken $P2X_5$ receptor. *J Neurochem* **77:**1256–1265.

Ryten M, Dunn PM, Neary JT, and Burnstock G (2002) ATP regulates the differentiation of mammalian skeletal muscle by activation of a $P2X_5$ receptor on satellite cells. *J Cell Biol* **158:**345–355.

Ryten M, Hoebertz A, and Burnstock G (2001) Sequential expression of three receptor subtypes for extracellular ATP in developing rat skeletal muscle. *Dev Dyn* **221:**331–341.

Spelta V, Jiang L-H, Surprenant A, and North RA (2002) Kinetics of antagonist actions at rat $P2X_{2/3}$ heteromeric receptors. *Br J Pharmacol* **135:**1524–1530.

Surprenant A, Rassendren F, Kawashima E, North RA, and Buell G (1996) The cytolytic P2Z receptor for extracellular ATP identified as a P2X receptor (P2X7). *Science (Wash DC)* **272:**735–738.

Surprenant A, Schneider DA, Wilson HL, Galligan JJ, and North RA (2000) (2000) Functional properties of heteromeric $P2X_{1/5}$ receptors expressed in HEK cells and excitatory junction potentials in guinea-pig submucosal arterioles. *J Autonom Nerv Syst* **81:**249–263.

Thomas SA and Hume RI (1990a) Irreversible desensitisation of ATP response in developing chick skeletal muscle. *J Physiol* **430:**373–388.

Thomas SA and Hume RI (1990b) Permeation of both cations and anions through a single class of ATP-activated channels in developing chick skeletal muscle. *J Gen Physiol* **95:**569–590.

Thomas SA, Zawisa MJ, Lin X, and Hume RI (1991) A receptor that is highly specific for extracellular ATP in developing chick skeletal muscle in vitro. *Br J Pharmacol* **103:**1963–1969.

Torres GE, Haines WR, Egan TM, and Voigt MM (1998) Co-expression of $P2X_1$ and $P2X_5$ receptor subunits reveals a novel ATP-gated ion channel. *Mol Pharmacol* **54:**989–993.

Urano T, Nishimori H, Han H-J, Furuhata T, Kimura Y, Nakamura Y, and Tokino

T (1997) Cloning of P2XM, a novel human P2X receptor gene regulated by p53. *Cancer Res* **57:**3281–3287.
Virginio C, MacKenzie A, North RA, and Surprenant A (1999a) Kinetics of cell lysis, dye uptake and permeability changes in cells expressing the rat $P2X_7$ receptor. *J Physiol* **519:**335–346.
Virginio C, MacKenzie A, Rassendren FA, North RA, and Surprenant A (1999b) Pore dilation of neuronal P2X receptor channels. *Nat Neurosci* **2:**315–321.
Virginio C, North RA, and Surprenant A (1998a) Calcium permeability and block at homomeric and heteromeric $P2X_2$ and $P2X_3$ receptors and receptors in rat nodose neurones. *J Physiol* **510:**27–35.
Virginio C, Robertson G, Surprenant A, and North RA (1998b) Trinitrophenyl substituted nucleotides are potent antagonists selective for $P2X_1$, $P2X_3$ and heteromeric $P2X_{2/3}$ receptors. *Mol Pharmacol* **53:**969–973.
Wells DG, Zawisa MJ, and Hume RI (1995) Changes in responsiveness to extracellular ATP in chick skeletal muscle during development and upon denervation. *Dev Biol* **172:**585–590.

Address correspondence to: R. Alan North, Institute of Molecular Physiology, University of Sheffield, Alfred Denny Building, Western Bank, Sheffield S10 2TN, UK. E-mail: r.a.north@sheffield.ac.uk